

High-Pressure Study on Electron Transport and Structure of $\text{Nd}_{0.55}\text{Sr}_{0.45}\text{MnO}_3$ and $\text{Nd}_{0.5}\text{Sr}_{0.5}\text{MnO}_3$

Congwu Cui,¹ Trevor A. Tyson,¹ and Zhong Zhong²

¹Physics Department, New Jersey Institute of Technology, Newark, New Jersey 07102

²National Synchrotron Light Source, Brookhaven National Laboratory, Upton, NY 11973

ABSTRACT

Pressure effects on the electron transport and structure of $\text{Nd}_{1-x}\text{Sr}_x\text{MnO}_3$ ($x = 0.45, 0.5$) were investigated in the range from ambient to ~ 6 GPa. In $\text{Nd}_{0.55}\text{Sr}_{0.45}\text{MnO}_3$, the low temperature ferromagnetic metallic state is suppressed and a low temperature insulating state is induced by pressure while in $\text{Nd}_{0.5}\text{Sr}_{0.5}\text{MnO}_3$, the CE-type antiferromagnetic charge ordering state is suppressed. Under pressure, both sample have a similar electron transport behavior although their ambient ground states are much different. We suggest the pressure induced magnetic state in both samples to be A-type antiferromagnetic.

PACS numbers: 62.50.+p, 71.27.+a, 75.25.+z, 75.47.Lx

In $\text{Nd}_{1-x}\text{Sr}_x\text{MnO}_3$ manganite, the size difference between Nd^{3+} and Sr^{2+} is large (~ 0.15 Å). By increasing Sr^{2+} concentration, the bandwidth is increased. With doping concentration change, interesting spin, charge and orbital phases are produced.¹ This doping system, especially at $x \sim 0.5$, has been extensively investigated.

In the $x = 0.5$ compound, on cooling from room temperature, there exist a transition from paramagnetic insulating (PMI) phase to ferromagnetic metallic (FMM) phase at ~ 255 K and a transition from FMM phase to charge ordering (CO) antiferromagnetic (AF) insulating (AFI) phase at ~ 155 K. The magnetic structure in CO AFI phase is CE-type.² With the application of a magnetic field, the FMM state is enhanced and the charge ordering state is suppressed and melts above 7 T.³ The magnetic field induced collapse of CO state is accompanied by a structural transition at which the volume increases drastically, leading to large positive magnetovolume effect.⁴ The orbital ordering (OO) coincides to charge ordering. Different orbital ordering types, $d_{3x^2-r^2}/d_{3y^2-r^2}$ -type⁵ or $d_{x^2-y^2}$ -type,⁶ have been suggested in this compound.

$\text{Nd}_{0.45}\text{Sr}_{0.55}\text{Mn}_3$ is an A-type antiferromagnetic metal with coupled magnetic and structure transition at ~ 225 K.² Spins are ferromagnetically aligned in ab-plane in Pbnm symmetry. Charge carriers are confined within ab-plane while the transport along c-axis is quenched, leading the resistivity to be highly anisotropic ($\rho_c/\rho_{ab} \sim 10^4$ at 35 mK).⁷ The antiferromagnetic spin ordering is accompanied by the $d_{x^2-y^2}$ -type orbital ordering, both of which can be simultaneously destructed by a high magnetic field, accompanied by a discontinuous decrease of resistivity.⁸

In this manganite system, the magnetic, electronic and orbital transitions are correlated to an abrupt structure transition, in which the a and b lattice constants are

elongated and c is compressed (in $Pbnm$ symmetry).⁷ Other groups showed that in $Nd_{0.5}Sr_{0.5}MnO_3$, during transition from FMM to AFI CO state, the crystal symmetry is lowered to monoclinic $P21/m$.^{9,10} Ritter *et al.*¹¹ suggested that the low temperature AFI CO phase is phase-segregated in two different crystallographic structures and three magnetic phases: orthorhombic ($Imma$) ferromagnetic, orthorhombic ($Imma$) A-type antiferromagnetic, and monoclinic ($P21/m$) charge-ordered CE-type antiferromagnetic phases, in which magnetic field can induce the charge-ordered monoclinic phase to collapse and to transform into FMM orthorhombic phase. Kajimoto *et al.*¹² showed that in CE-type and A-type AF state, the MnO_6 octahedra are apically compressed corresponding to $d_{3x^2-r^2}/d_{3y^2-r^2}$ or $d_{x^2-y^2}$ orbital ordering.

Hydrostatic and uniaxial pressure affect CO and FMM states differently. In $Nd_{0.5}Sr_{0.5}MnO_3$, hydrostatic pressure ($<\sim 1$ GPa) increases T_C at 6.8 K/GPa and decrease T_{CO} at 8.4 K/GPa,¹³ while the uniaxial pressure along c -axis increases T_{CO} at 0.19 K/MPa and decreases T_C at 0.06 K/MPa.¹⁴ In $Nd_{0.45}Sr_{0.55}MnO_3$, by applying uniaxial pressure along c -axis, the A-type antiferromagnetic phase is stabilized by increasing T_N at 0.066 K/MPa, which may imply the stabilization of the $d_{x^2-y^2}$ orbital.¹⁴ In thin films, due to the effect of substrate, biaxial strain is induced, which is an analogy to uniaxial pressure. In $Nd_{0.5}Sr_{0.5}MnO_3$ thin films, the thickness mediates the competition between CO insulating and FMM state,¹⁵ and there is an optimal strain for both CO and metallic state appearing in this material.¹⁶

The correlation between structure and electronic and magnetic transitions indicates its crucial role in this doping system. By applying high pressure up to ~ 6 GPa, we studied the CO, FMM, AFM state changes in $Nd_{0.55}Sr_{0.45}MnO_3$ and $Nd_{0.5}Sr_{0.5}MnO_3$ through

resistivity and structure measurements. It is found that pressure induces a similar electronic and magnetic behavior in them, which can be partly correlated to the orthorhombic distortion changes under pressure.

The samples were prepared by solid-state reaction. Stoichiometric amount of Nd_2O_3 , MnO_2 , and SrCO_3 powder were mixed. After multiple grinding and calcinations, the powder was pressed into pellets. The pellets were sintered and annealed. The x-ray diffraction patterns show a single crystallographic phase. The magnetization and resistivity measurements are consistent to the results of other groups.^{1,17,18} The details of high-pressure resistivity and structure measurement methods were described elsewhere.¹⁹

$\text{Nd}_{0.55}\text{Sr}_{0.45}\text{MnO}_3$ is a double exchange compound, with a FMM to PMI transition at ~ 280 K upon warming. Under pressure, the electron transport is modified interestingly. FIG. 1(a) is the resistivity as a function of temperature at several typical pressures. The most salient feature is the insulating state arising in low temperature range under pressure. With pressure increase, the insulating behavior dominates above ~ 6 GPa. Consequently, resistivity in measured temperature range changes with pressure [inset of FIG. 2(a)]. Below ~ 3.5 GPa, the resistivity in PMI phase is reduced while in FMM phase is almost unchanged. Above ~ 3.5 GPa, in both phases, resistivity increases fast with pressure. In low-pressure range, the metal-insulator transition temperature T_{MI} increases with pressure. Due to the limit of instrument, T_{MI} above instrument upper limit in range of ~ 2 -4 GPa cannot be determined. Above ~ 4 GPa, the transition temperature decreases on pressure increasing. Above ~ 6 GPa, the insulating behavior dominates so that the transition temperature can not be determined, although there is still obvious trace of metallic behavior. The transition temperature change under pressure is plotted in FIG.

2(a). The third-order fitting gives a critical pressure $P^* \sim 2.6$ GPa, while the resistivity in paramagnetic phase (at ~ 316 K) gives $P^* \sim 3.6$ GPa [inset of FIG. 2(a)].

In this compound, the behavior of T_{MI} and resistivity is similar to that found in manganites of $La_{0.60}Y_{0.07}Ca_{0.33}MnO_3$ ¹⁹ and $Pr_{0.7}Ca_{0.3}MnO_3$.²⁰ However, the mechanism that the material becomes insulating at high pressures is different. In those two compounds, the material become insulating through the suppression of FMM state, displaying as the T_{MI} decreasing above critical pressure. In $Nd_{0.55}Sr_{0.45}MnO_3$, the insulating state at high pressures comes from two aspects: the suppression of FMM state and the expanding of a low temperature insulating phase, which appears with pressure increasing and finally dominates at high pressures. While the material becomes insulating under pressure, the enhancement of insulating component contributes mostly.

Abramovich *et al.*²¹ proposed phase-separation model in which the AFI droplets lie in the conducting FM host. In the phase-separation model, the behavior of the material becoming insulating can be understood as pressure induced percolation that the increasing pressure suppresses FMM component and enhances AFI component above P^* .

It is noted that the transport behavior at high pressures where the compound becomes insulating is very similar to that of $Nd_{0.45}Sr_{0.55}MnO_3$ at ambient pressure.²² When applied a high magnetic field of 35 T, resistivity of the A-type AF metallic $Nd_{0.45}Sr_{0.55}MnO_3$ becomes similar to that of $Nd_{0.55}Sr_{0.45}MnO_3$, which is ascribed to the destruction of A-type AFM spin ordering and $d_{x^2-y^2}$ orbital ordering.⁸ Considering the similarity between the resistivity of $x = 0.45$ compound under high pressure and $x = 0.55$ at ambient pressure and that of $x = 0.55$ in high magnetic field, one might speculate that the state induced by pressure in $x = 0.45$ compound has a similar spin and orbital

structure to $\text{Nd}_{0.45}\text{Sr}_{0.55}\text{MnO}_3$.

In FIG. 3(a), the compressibilities of lattice parameters are shown. The different compressibility leads to further distortion of the unit cell. To describe the orthorhombic distortion, Meneghini *et al.*²³ defined the orthorhombic strain in ab-plane ($Os_{ab} = 2\frac{a-b}{a+b}$) and along c-axis ($O_c = 2\frac{a+b-c\sqrt{2}}{a+b+c\sqrt{2}}$) (in Pbnm symmetry). When the lattice is cubic, both Os_{ab} and O_c are zero. FIG. 3(b) shows that both strains increase under pressure, indicating a more distorted structure from the cubic case.

The structure of $\text{Nd}_{0.45}\text{Sr}_{0.55}\text{MnO}_3$ is O^\dagger with $a \approx b < \frac{c}{\sqrt{2}}$. The corresponding orthorhombic strain in ab-plane is ~ 0 , along c-axis is -2% (calculated with the data in ref. 12), which corresponds to the $d_{x^2-y^2}$ -type orbital ordering and A-type AFM metal state. Under pressure, the orthorhombic strain in both c-axis and ab-plane is increased in $\text{Nd}_{0.55}\text{Sr}_{0.45}\text{MnO}_3$, indicating that the high pressure structure is more different from $\text{Nd}_{0.45}\text{Sr}_{0.55}\text{MnO}_3$ than at ambient pressure. This ab-plane strain increasing implies that the orbital state is different. However, the similarity between the resistivity (in both absolute value and shape) seems to suggest an A-type antiferromagnetic state induced by pressure in $\text{Nd}_{0.55}\text{Sr}_{0.45}\text{MnO}_3$.

FIG. 1(b) is the resistivity of $\text{Nd}_{0.5}\text{Sr}_{0.5}\text{MnO}_3$ under pressure. In the low temperature CO AFI phase, the resistivity is reduced by pressure. On the other hand, the insulating manner extends to higher temperature so that the FM metallic state is suppressed. If we define the temperature where insulating and metallic state cross (the resistivity minimum) as CO transition, T_{CO} increases with pressure and it seems to

decrease above ~ 4 GPa [FIG. 2(b)]. In the mean time, pressure affects the metal-insulator transition slightly. With pressure increase, T_{MI} increases below ~ 3 GPa and drops above ~ 3 GPa. The highest T_{MI} is only ~ 4 K difference from ambient pressure. In measured pressure range, resistivity in PMI is suppressed.

That T_{CO} increases with pressure below ~ 3.8 GPa while T_{MI} almost does not change [FIG. 2(b)] is different from that hydrostatic pressure (< 1 GPa) increases T_C and decrease T_{CO} reported by other authors.¹³ On the contrary, our results are similar to the effects of uniaxial pressure along c-axis.¹⁴ Under pressure, it was found that the c-axis strain increases while ab-plane strain decreases with pressure [FIG. 3(c) and (d)]. Because the CO state corresponds to a higher orthorhombic strain state,³ possibly the pressure induced c-axis strain increase enhances the CO state. On the other hand, the slight ab-plane strain decrease may enhance the electron hoping and lead to the resistivity decrease in the ab-plane.

Roy *et al.*²⁴ reported that pressure above ~ 1.5 GPa can split the coincident antiferromagnetic and charge ordering transitions in which T_{CO} increases while T_N decreases. With the transitions decoupled, resistivity rises abruptly at the magnetic transition but not at CO transition, implying that low temperature resistivity comes mostly from the CE-type antiferromagnetic state but not the charge ordering state. We did not observe the T_{CO} and T_N splitting in a larger pressure range, possibility because our sample is polycrystalline. However, the large suppression of resistivity indicates that the antiferromagnetic state, specifically the CE-type AF state, is suppressed, which is also consistent to the ab-plane orthorhombic strain reduction [FIG. 3(d)].

In $Nd_{0.5}Sr_{0.5}MnO_3$, by substituting Nd^{3+} with larger size La^{3+} , the bandwidth is

increased and hence the CO phase is suppressed while T_C increasing. When applied pressure, a transition from CO CE-type AFI to A-type AFI was suggested, in which resistivity is suppressed and T_{CO} gradually increases with pressure.²⁵ This is consistent to our result in the small bandwidth parent compound but at a much higher pressure. The smaller ab-plane strain and larger c-axis strain at high pressures may favor an A-type AF state and $d_{x^2-y^2}$ orbital ordering as in the $x = 0.55$ compound. In this A-type AFI state, resistivity is decreased due to enhanced in-plane transfer integral by the reduction of in-plane strain. In the phase-separation model,¹¹ the A-type AF phase is enhanced and the CO CE-type AF phase is suppressed concomitantly by pressure. Because bandwidth is sensitive to the local atom structure of MnO_6 octahedra, especially the Mn-O-Mn bond angle, it is highly desired to measure the local atomic structure to explain the electronic and magnetic behavior under pressure.

The two $Nd_{1-x}Sr_xMnO_3$ manganites at $x = 0.45$ and 0.5 have very different electronic, magnetic and orbital ground states at ambient conditions. However, when we compare the resistivity at high pressure, we can find a surprising similarity between them [FIG. 1 (a) and (b)]. FIG. 4 is an example of the resistivity of these two compounds at pressures above the critical pressure. The similarity also seems to imply a similar electronic and magnetic state. The structure measurements partly justify this assumption. The orthorhombic strain of $x = 0.45$ is increased by pressure to almost same as that of the $x = 0.5$ compound at ambient pressure [FIG. 3(b) and (d)]. In addition, the similarity between the high pressure resistivity of these two compounds and that of $Nd_{0.45}Sr_{0.55}MnO_3$ also suggests an A-type AFI phase in the high pressure phase.

It is interesting to compare the effects of pressure and strain in thin films. The inset

of FIG. 4 is the resistivity of $\text{Nd}_{0.5}\text{Sr}_{0.5}\text{MnO}_3$ thin films of several typical thickness from Prellier *et al.*¹⁵ With thickness decreasing, the strain in thin films is regarded to increase. Compared with $\text{Nd}_{0.55}\text{Sr}_{0.45}\text{MnO}_3$, the resistivity evolution with thickness decrease (strain increase) is an analogy to pressure increase in bulk $\text{Nd}_{0.55}\text{Sr}_{0.45}\text{MnO}_3$, indicating that pressure increases strain in bulk sample proved by structure measurements.

In summary, by studying the resistivity and structure of $\text{Nd}_{1-x}\text{Sr}_x\text{MnO}_3$ ($x = 0.45, 0.5$), it is found that they have a similar resistivity as a function of temperature, which results from the different effect of pressure on structure. Under pressure, both the ferromagnetic metallic state in the $x = 0.45$ compound and the CE-type antiferromagnetic insulating state in the $x = 0.5$ compound are suppressed. By comparing the resistivity and structure with the $x = 0.55$ compound, pressure appears to induce a similar electronic and magnetic state in these two much different compounds. We suggest that the pressure induced magnetic states in both samples are A-type antiferromagnetic.

The high pressure x-ray diffraction measurements were performed at beamline X17B1, NSLS, Brookhaven National Laboratory which is supported by US Department of Energy contract DE-AC02-76CH00016. The authors would like to thank Dr. Jingzhu Hu at X17C, NSLS for her help on the pressure calibration for x-ray diffraction. This work is supported by National Science Foundation Career Grant DMR-9733862 and by DMR-0209243.

CAPTIONS

FIG. 1 Resistivity of $\text{Nd}_{0.55}\text{Sr}_{0.45}\text{MnO}_3$ and $\text{Nd}_{0.5}\text{Sr}_{0.5}\text{MnO}_3$ under pressure.

FIG. 2 Transition temperatures of $\text{Nd}_{0.55}\text{Sr}_{0.45}\text{MnO}_3$ (a) and $\text{Nd}_{0.5}\text{Sr}_{0.5}\text{MnO}_3$ (b). The solid lines are third-order polynomial fittings for eye guiding. (a) Metal-insulator transition temperature of $\text{Nd}_{0.55}\text{Sr}_{0.45}\text{MnO}_3$, the inset is the resistivity changes with pressure in PMI phase [at 316 K (solid circle) and FMM phase [at 120 K (open circle)]; (b) Metal-insulator transition (solid circle) and charge ordering transition (solid square) temperature of $\text{Nd}_{0.5}\text{Sr}_{0.5}\text{MnO}_3$.

FIG. 3 Compressibility of lattice parameters and orthorhombic strain of $\text{Nd}_{0.55}\text{Sr}_{0.45}\text{MnO}_3$ and $\text{Nd}_{0.5}\text{Sr}_{0.5}\text{MnO}_3$. Left panel: compressibility of lattice parameters (a) and the ab-plane and c-axis orthorhombic strain (b) of $\text{Nd}_{0.55}\text{Sr}_{0.45}\text{MnO}_3$; right panel: compressibility of lattice parameters (c) and ab-plane and c-axis orthorhombic strain (d) of $\text{Nd}_{0.5}\text{Sr}_{0.5}\text{MnO}_3$. The solid lines in (a) and (c) are eye guides. (The definition of the orthorhombic strain is in text)

FIG. 4 Comparison of resistivity of $\text{Nd}_{0.55}\text{Sr}_{0.45}\text{MnO}_3$ and $\text{Nd}_{0.5}\text{Sr}_{0.5}\text{MnO}_3$ under pressure. The inset is the resistivity of $\text{Nd}_{0.5}\text{Sr}_{0.5}\text{MnO}_3$ thin films with different thickness from ref. 15 for comparison to our pressure results.

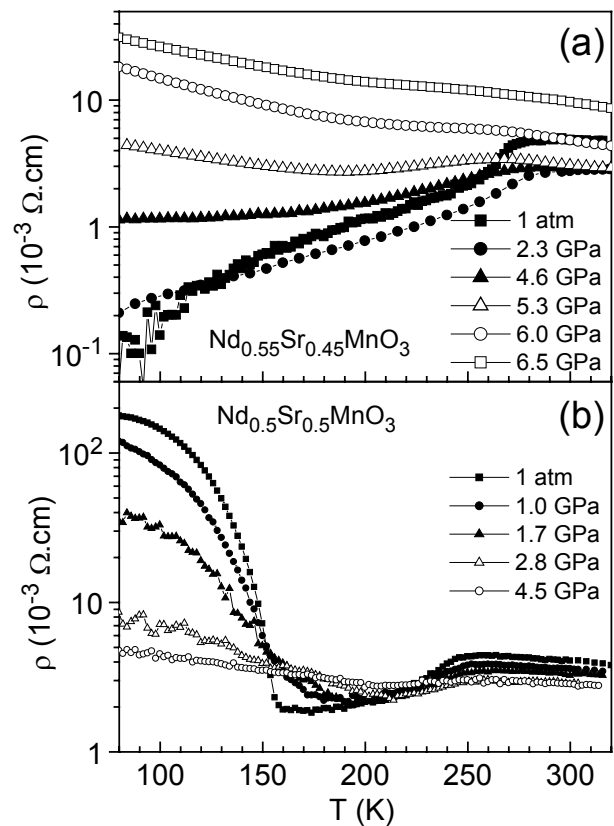


FIG. 1-CUI

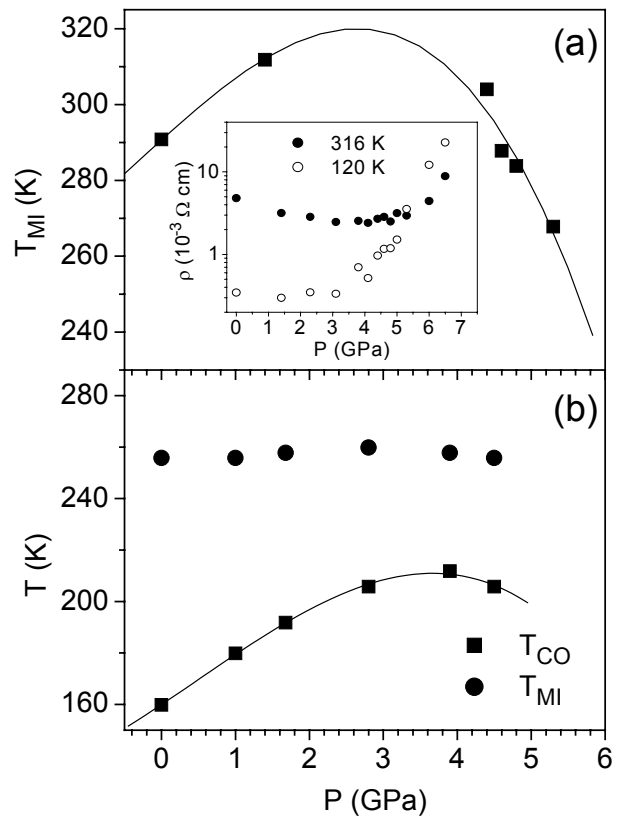


FIG. 2-CUI

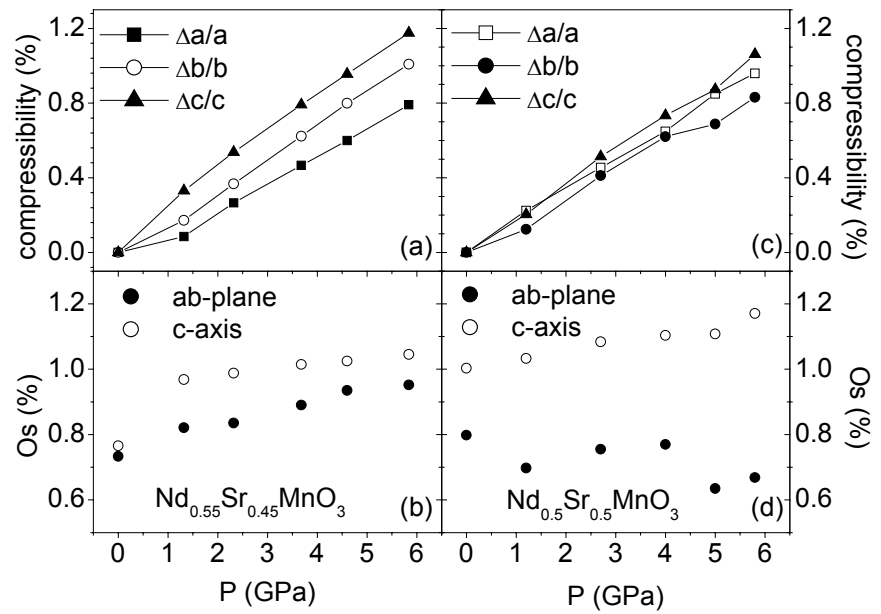


FIG. 3-CUI

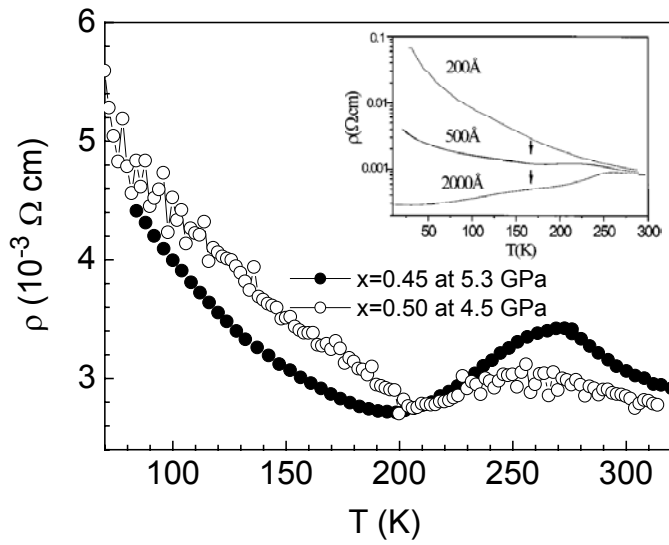


FIG. 4-CUI

REFERENCES

¹ Y. Tokura and Y. Tomioka, J. of Magn. and Magn. Mat. **200**, 1 (1999).

² H. Kawano, R. Kajimoto, H. Yoshizawa, Y. Tomioka, H. Kuwahara and Y. Tokura, Phys. Rev. Lett. **78**, 4253 (1997).

³ H. Kuwahara, Y. Tomioka, and A. Asamitsu *et al.*, Science **270**, 961(1995).

⁴ R. Mahendiran, M. R. Ibarra, and A. Maignan *et al.*, Phys. Rev. Lett. **82**, 2191 (1999).

⁵ K. Nakamura, T. Arima, and A. Nakazawa *et al.*, Phys. Rev. B **60**, 2425 (1999).

⁶ S. Zvyagin, A. Angerhofer, and K. V. Kamenev *et al.*, Solid State Commun. **121**, 117 (2002).

⁷ H. Kuwahara, T. Okuda, Y. Tomioka, T. Kimura, A. Asamitsu, and Y. Tokura, Mat. Res. Soc. Symp. Proc. 494, 83 (1998).

⁸ T. Hayashi, N. Miura and K. Noda *et al.* Phys. Rev. B 65, 024408 (2002).

⁹ V. Eremenko, S. Gnatchenko and N. Makedonska *et al.*, Fizika Nizkikh Temperatur 27,1258 (2001).

¹⁰ P. Laffez, G. Van Tendeloo, f. Millange, V. Caignaert, M. Hervieu and B. Raveau, Mater. Res. Bull. 31, 905 (1996).

¹¹ C. Ritter, R. Mahendiran, M. R. Ibarra, L. Morellon, A. Maignan, B. Ravea and C. N. R. Rao, Phys. Rev. B 61, R9229 (2000).

¹² R. Kajimoto, H. Yoshizawa, H. Kawano, H. Kuwahara, Y. Tokura, K. Ohoyama and M. Ohashi, Phys. Rev. B **60**, 9506 (1999).

¹³ Y. Moritomo, H. Kuwahara, and Y. Tokura, J. Phys. Soc. Jpn. **66**, 556 (1997).

¹⁴ Taka-hisa Arima and Kenji Nakamura, Phys. Rev. B **60**, R15013 (1999).

¹⁵ W. Prellier, A. Biswas, and M. Rajeswari *et al.*, *Appl. Phys. Lett.* **75**, 397 (1999).

¹⁶ Q. Qian, T. A. Tyson, and C.-C. Kao *et al.*, *Phys. Rev. B* **63**, 224424 (2001).

¹⁷ V. Caignaert, F. Millange, M. Hervieu, E. Suard, and B. Raveau, *Solid State Commun.* **99**, 173 (1996).

¹⁸ Y. Tomioka, H. Kuwahara, A. Asamitsu, M. Kasai, and Y. Tokura, *Appl. Phys. Lett.* **70**, 3609 (1997).

¹⁹ Congwu Cui, Trevor A. Tyson, Zhong Zhong, Jeremy P. Carlo, and Yuhai Qin, *Phys. Rev. B* **67**, 104107 (2003).

²⁰ Congwu Cui and Trevor A. Tyson, unpublished.

²¹ A. I. Abramovich, A. V. Michurin, O. Yu Gorbenko, and A. R. Kaul, *J. Phys.: Condens. Matter* **12**, L627 (2000).

²² H. Kuwahara1, T. Okuda, and Y. Tomioka *et al.*, *Phys. Rev. Lett.* **82**, 4316 (1999)

²³ C. Meneghini, D. Levy and S. Mobilio M. Ortolani, M. Nuñez-Reguero, Ashwani Kumar, and D. D. Sarma, *Phys. Rev. B* **65**, 012111 (2001).

²⁴ A. S. Roy, A. Husmann, T. F. Rosenbaum, and J. F. Mitchell, *Phys. Rev. B* **63**, 094416 (2001)

²⁵ Y. Moritomo, H. Kuwahara, Y. Tomioka, and Y. Tokura, *Phys. Rev. B* **55**, 7549 (1997).